

Electronic Supplementary Information

for

**Catalytic interconversion between hydrogen and formic acid at
ambient temperature and pressure**

Yuta Maenaka, Tomoyoshi Suenobu and Shunichi Fukuzumi*

X-ray crystallographic studies

Crystallographic data for **2** has been deposited with the Cambridge Crystallographic Data Center as Supplementary Publication No. 814147. This data can be obtained free of charge from the Cambridge Crystallographic Data Center via www.ccdc.cam.ac.uk/data_request/cif. The intensity data sets were collected on Rigaku AFC-8 X-ray diffractometers with graphite monochromated Mo- K_{α} radiation ($\lambda = 0.71073 \text{ \AA}$) using a ω scan technique. CrystalClear software was used for data reduction and empirical absorption corrections. The structures were solved by the direct methods using the Siemens SHELXTLTM Version 5 package of crystallographic software. The difference Fourier maps based on these atomic positions yield the other non-hydrogen atoms. The hydrogen atom positions were generated theoretically, allowed to ride on their respective parent atoms and included in the structure factor calculations with assigned isotropic thermal parameters. The structures were refined using a full-matrix least-squares refinement on F^2 . All atoms except for hydrogen atoms were refined anisotropically. Crystal data for **2** are given in Table S1.

Table S1 X-ray crystallographic data for **2**¹

	2
formula	C ₂₀ H ₂₁ IrN ₂ O ₃
fw	529.62
crystal system	Monoclinic
space group	$P2_1/n$
T , K	123
a , Å	11.533(3)
b , Å	10.250(3)
c , Å	15.157(4)
β , deg	102.2719(10)
V , Å ³	1750.9(8)
Z	4
No. of reflections	12694
No. of observed reflections	3948

parameters	236
$R1^a$	0.0362 ($I > 2.0\sigma(I)$)
$wR2^b$	0.0979 (all data)
GOF	1.076

$$^a R1 = \sum ||F_o| - |F_c|| / \sum |F_o|. \quad ^b wR2 = [\sum (w(F_o^2 - F_c^2)^2) / \sum w(F_o^2)^2]^{1/2}$$

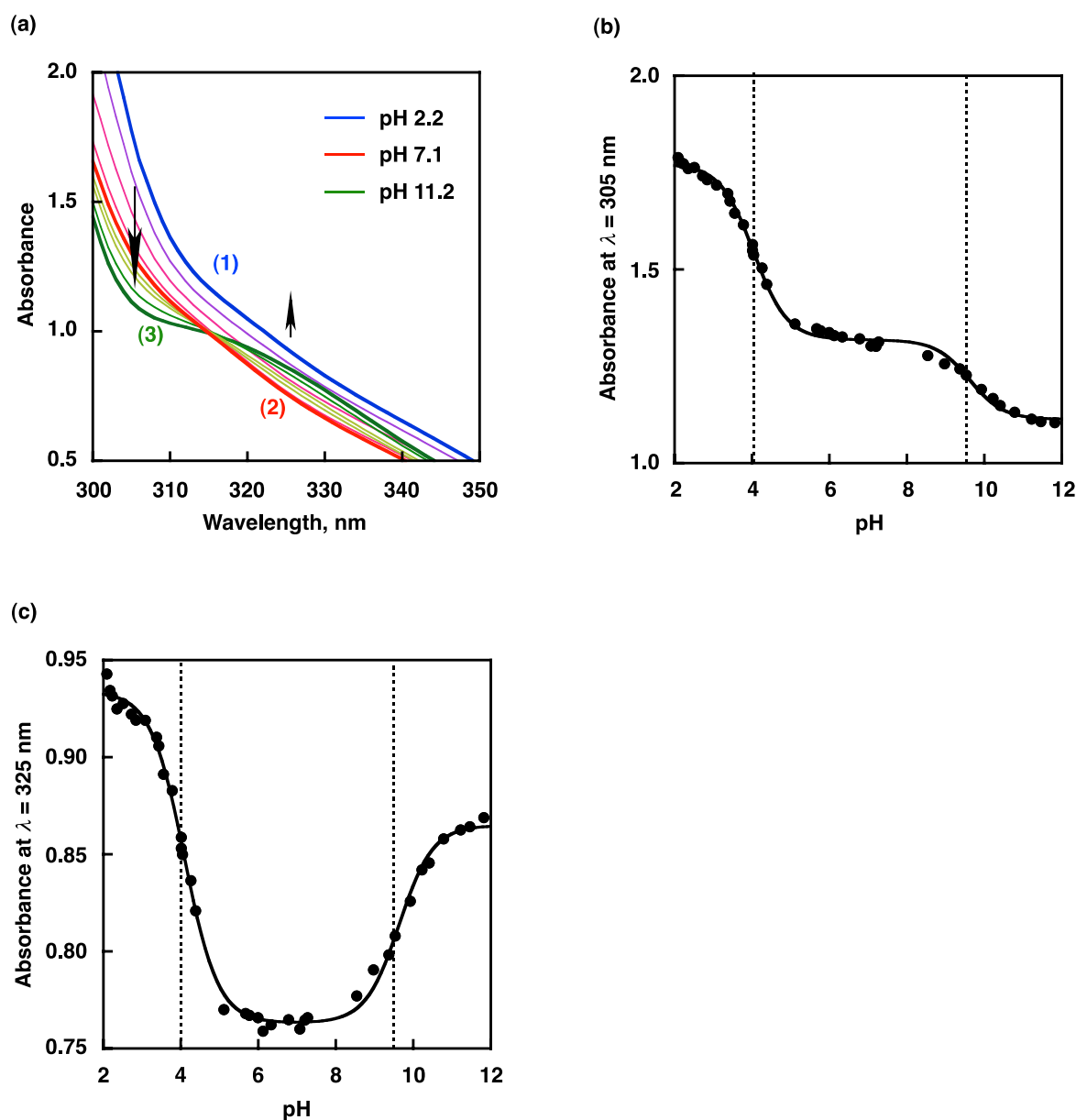


Fig. S1 (a) UV-vis spectral changes of $[1]_2 \cdot \text{SO}_4$ (70 μM) by the addition of NaOH (10 mM) in deaerated H_2O at 298 K at pH 2.2 (1, blue line), 7.1 (2, red line) and 11.2 (3, green line). (b) Change in absorbance at $\lambda = 305 \text{ nm}$ by the addition of NaOH (10 mM) in deaerated H_2O at 298 K (1 cm light-path length). (c) Change in absorbance at $\lambda = 325 \text{ nm}$ by the addition of NaOH (10 mM) in deaerated H_2O at 298 K (1 cm light-path length).¹

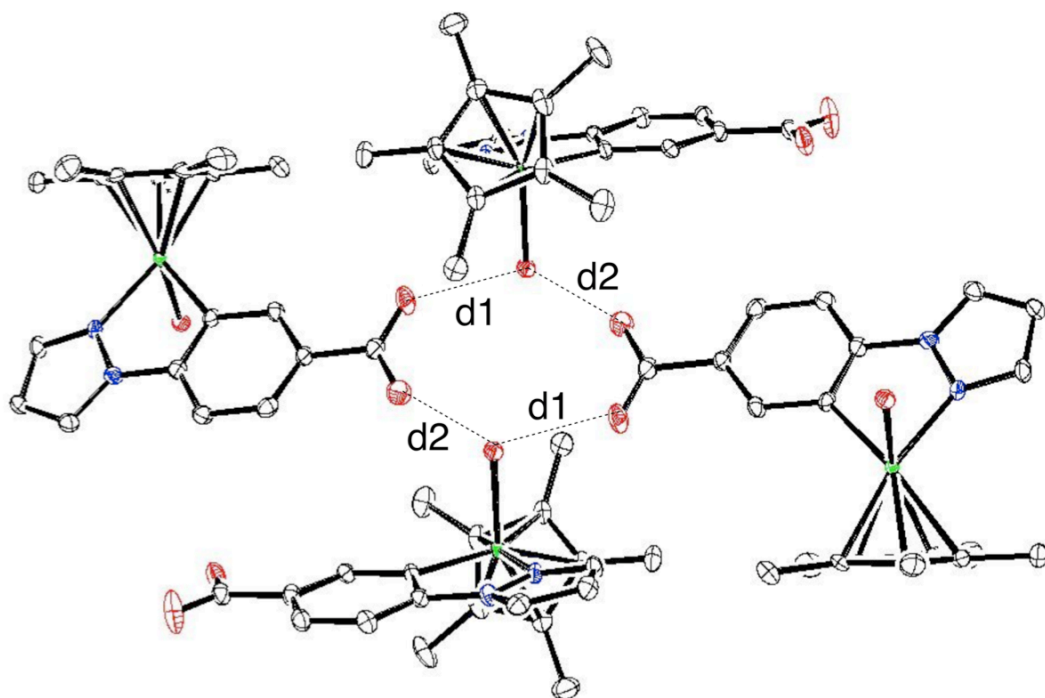


Fig. S2 ORTEP drawing of **2**. Hydrogen atoms are omitted for clarity. Selected bond length (Å): d1 = 2.590(4) and d2 = 2.560(4).¹

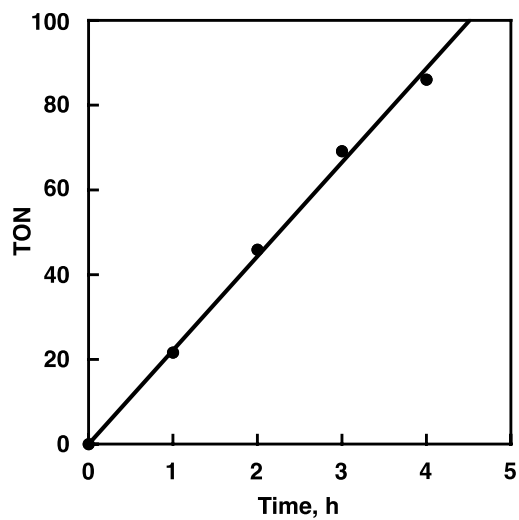


Fig. S3 Time course of TON for the formate formation in the hydrogenation of bicarbonate catalysed by **2** (0.26 mM) under atmospheric pressure of H₂ and CO₂ in deaerated H₂O at 333 K at pH 7.5.

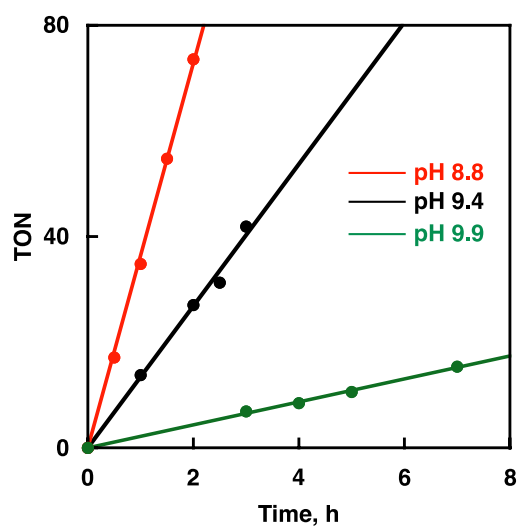


Fig. S4 Time course of TON for the formate formation under an atmospheric pressure of hydrogen catalysed by **2** (0.18 mM) in a deaerated $\text{KHCO}_3/\text{K}_2\text{CO}_3$ solution ($[\text{KHCO}_3] + [\text{K}_2\text{CO}_3] = 2.0 \text{ M}$) at 303 K at pH 8.8 (red line), 9.4 (black line) and 9.9 (green line), respectively.

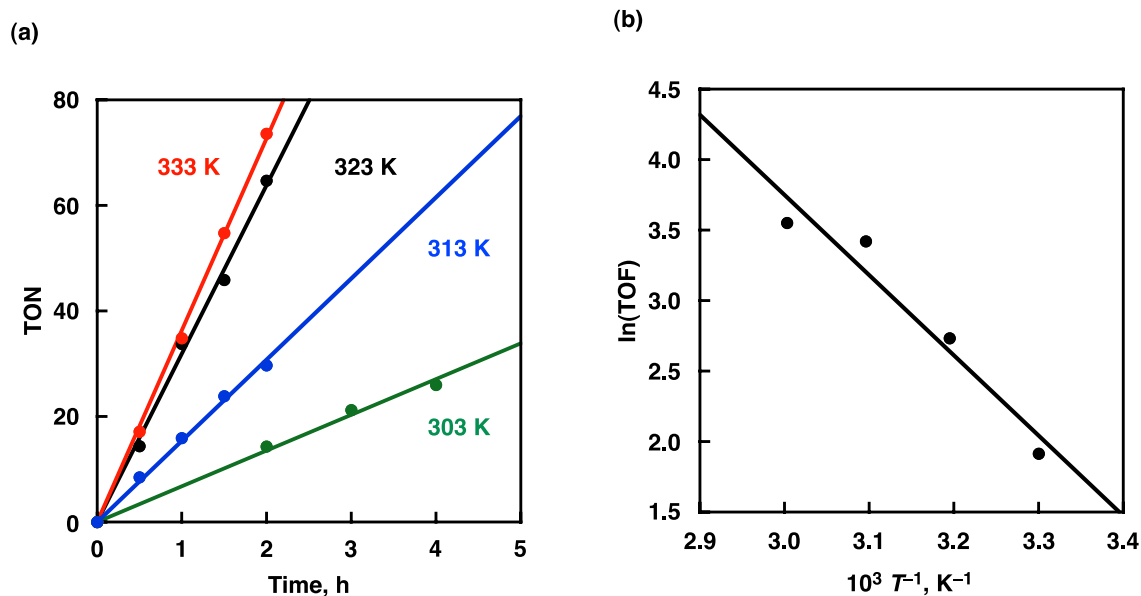


Fig. S5 (a) Time course of TON for the formate formation under an atmospheric pressure of hydrogen catalysed by **2** (0.18 mM) in a deaerated KHCO₃ (2.0 M) solution at pH 8.8 at 333 K (red line), 323 K (black line), 313 K (blue line) and 303 K (green line). (b) Arrhenius plot of TOF of the formate formation (TOF, h⁻¹) under an atmospheric pressure of hydrogen catalysed by **2** (0.18 mM) in a KHCO₃ (2.0 M) solution.

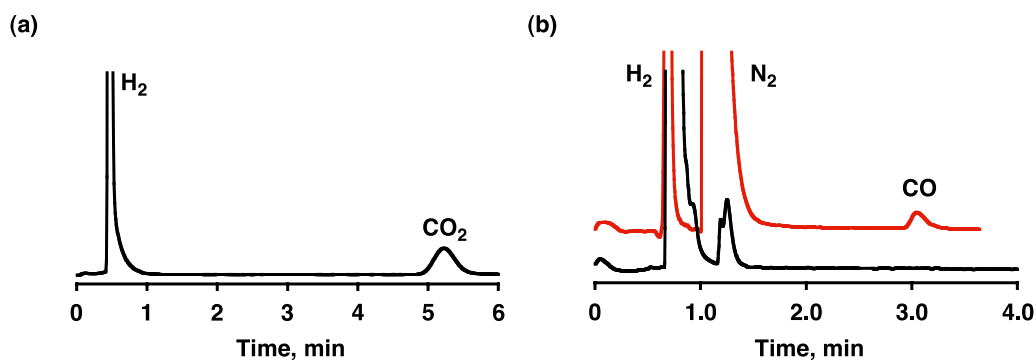


Fig. S6 (a) Gas chromatogram of the evolved gas (100 μL) in the decomposition of HCOOH/HCOOK ([HCOOH] + [HCOOK] = 3.3 M) catalysed by **1** (0.2 mM) after 5 min in deaerated H₂O at pH 2.8 at 293 K (b) Gas chromatogram of commercially available standard gas containing 1.06% CO (1000 μL, red line) and the evolved gas (1000 μL, black line) in the decomposition of HCOOH/HCOOK ([HCOOH] + [HCOOK] = 3.3 M) catalysed by **1** (0.2 mM) after 1 h in deaerated H₂O at pH 2.8 at 293 K

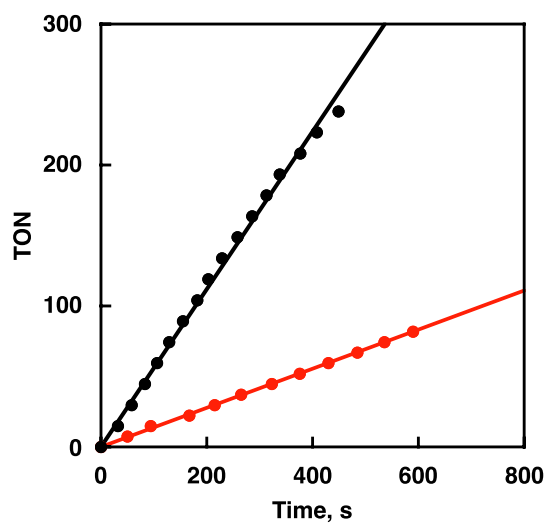


Fig. S7 Time course of TON for the decomposition of formic acid catalyzed by **1** (0.20 mM) in a deaerated HCOOH/HCOOK solution ($[\text{HCOOH}] + [\text{HCOOK}] = 3.3 \text{ M}$ in H_2O , black line) and DCOOH/DCOOK solution ($[\text{DCOOH}] + [\text{DCOOK}] = 3.3 \text{ M}$ in H_2O , red line) at pH 2.8 at 298 K.

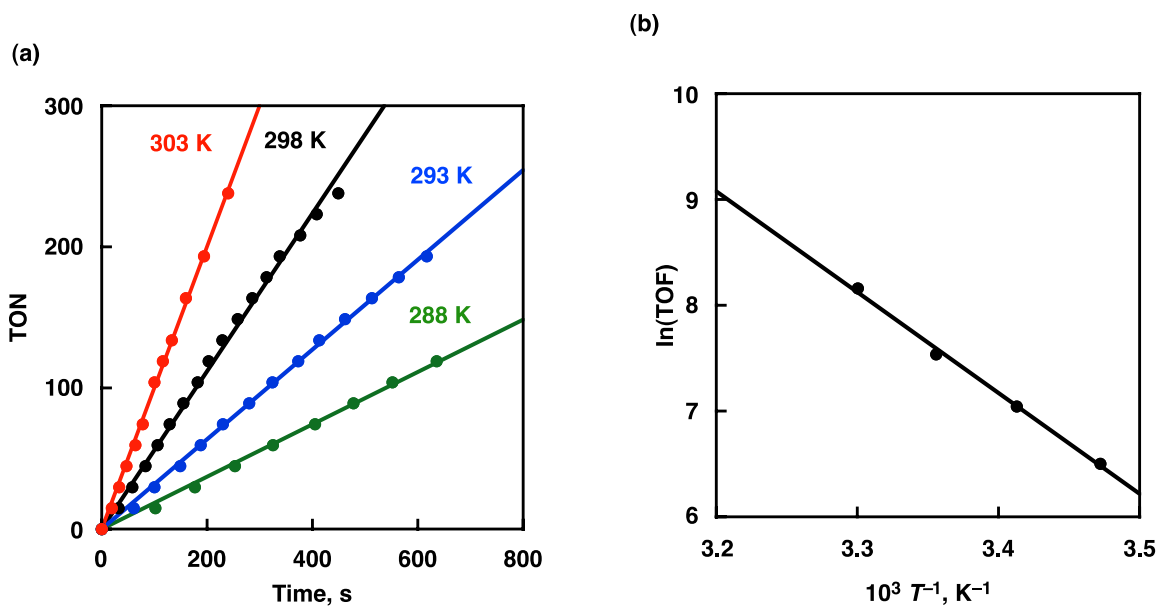


Fig. S8 (a) Time course of TON for the decomposition of formic acid catalysed by **1** (0.20 mM) in a deaerated HCOOH/HCOOK solution ($[\text{HCOOH}] + [\text{HCOOK}] = 3.3 \text{ M}$) at pH 2.8 at 303 K (red line), 298 K (black line), 293 K (blue line) and 288 K (green line). (b) Arrhenius plot of TOF of H₂ evolution for the decomposition of HCOOH/HCOOK ($[\text{HCOOH}] + [\text{HCOOK}] = 3.3 \text{ M}$) catalysed by **1** (0.20 mM) in a deaerated aqueous solution at pH 2.8.

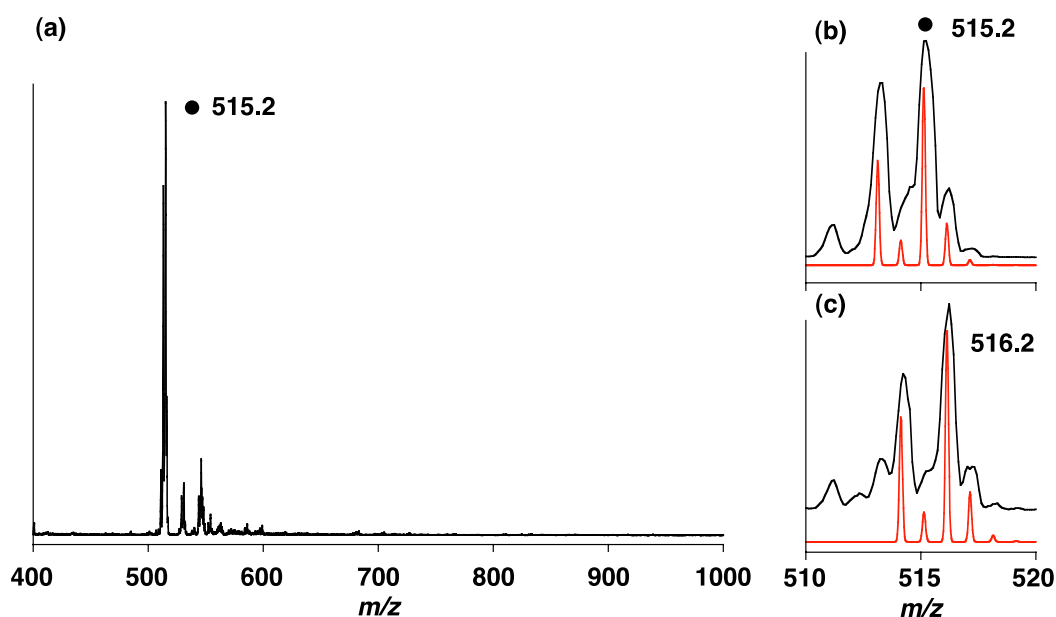


Fig. S9 (a) Negative-ion ESI mass spectrum of a mixed solution of a 1.5 μM NaOH aqueous solution and MeCN [1:1 (v/v)] containing compound **6** in the range of m/z 400 to 1000. The hydride complex **6** was prepared by bubbling a mixed solution of a 1.5 μM NaOH aqueous solution and MeCN [1:1 (v/v)] containing compound **2** (0.14 μM) with an atmospheric pressure of hydrogen. (b) The signal in the range of m/z 510 to 520 (black line) and the calculated isotopic distribution for **6** (red line). (c) Negative-ion ESI mass spectrum of a mixed solution of a 1.5 μM NaOH aqueous solution and MeCN [1:1 (v/v)] containing $[\text{Ir}^{\text{III}}(\text{Cp}^*)(4-(1H\text{-pyrazol-1-yl-}\kappa\text{N}^2)\text{benzonate-}\kappa\text{C}^3)\text{D}]^-$ **8** in the range of m/z 510 to 520 (black line) and the calculated isotopic distribution for **8** (red line). The hydride complex **8** was prepared by bubbling a mixed solution of a 1.5 μM NaOH aqueous solution and MeCN [1:1 (v/v)] containing compound **2** (0.14 μM) with an atmospheric pressure of D_2 gas at room temperature. The signals at m/z 511, m/z 512 and m/z 513 are assignable to the calculated isotopic distribution of the dehydrogenated **8**, i.e., $[\mathbf{2}-\text{H}_3\text{O}^+]^-$.¹

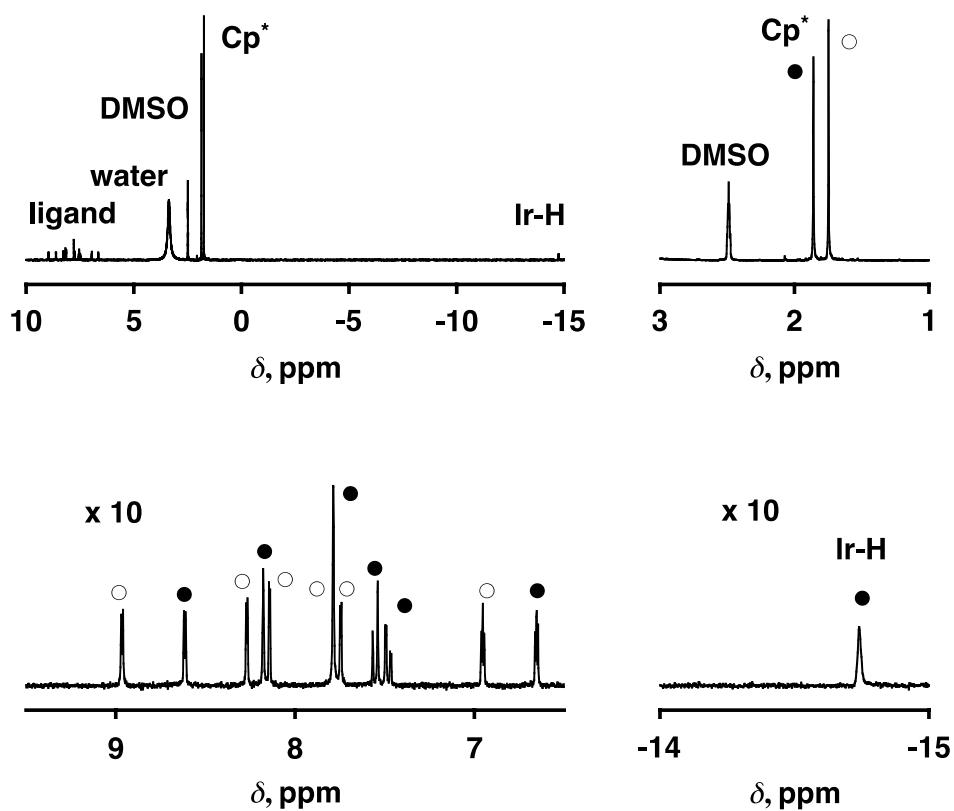


Fig. S10 ^1H NMR spectrum (upper left) and its magnified spectra of $[\text{Ir}^{\text{III}}(\text{Cp}^*)(4-(1H\text{-pyrazol-1-yl-}\kappa\text{N}^2)\text{benzoic acid-}\kappa\text{C}^3)\text{H}]$ (**5**, ●) and $[\text{Ir}^{\text{III}}(\text{Cp}^*)(4-(1H\text{-pyrazol-1-yl-}\kappa\text{N}^2)\text{benzoic acid-}\kappa\text{C}^3)(\text{H}_2\text{O})]_2\text{SO}_4$ (**1**, ○) in $\text{DMSO-}d_6$ at 298 K. The peak at $\delta = 2.50$ ppm is assignable to the methyl proton of DMSO contained in $\text{DMSO-}d_6$.

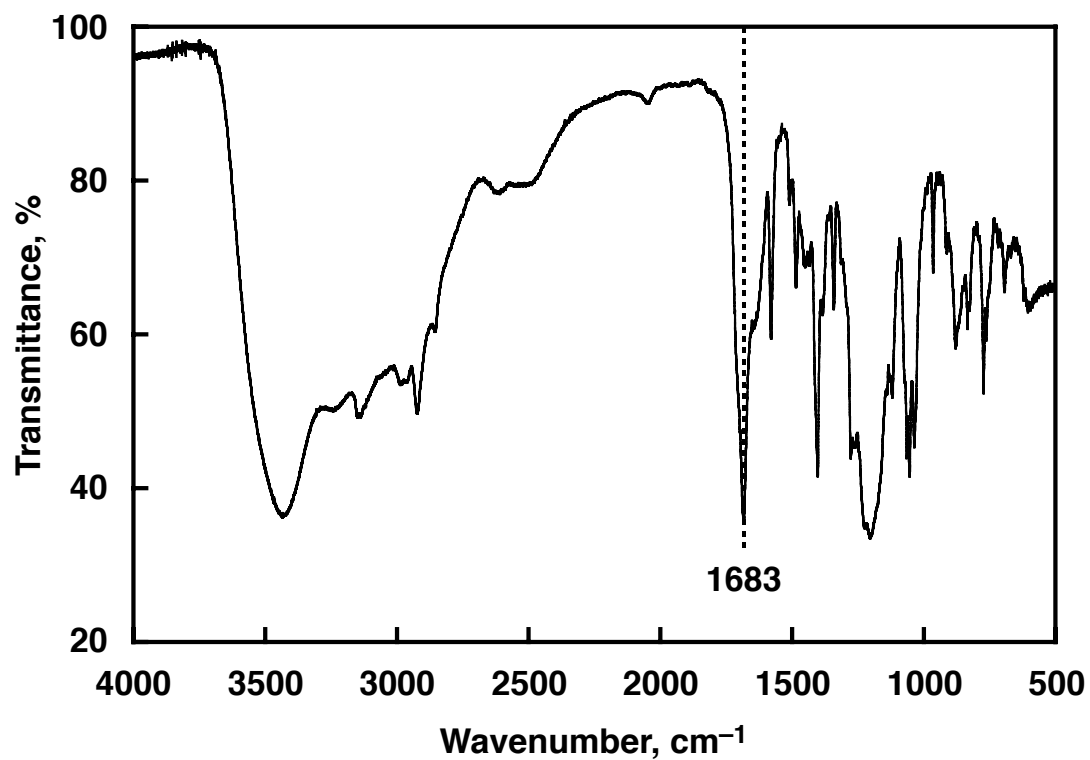


Fig. S11 IR spectrum of $[1]_2 \cdot \text{SO}_4$ diluted in a KBr disk.

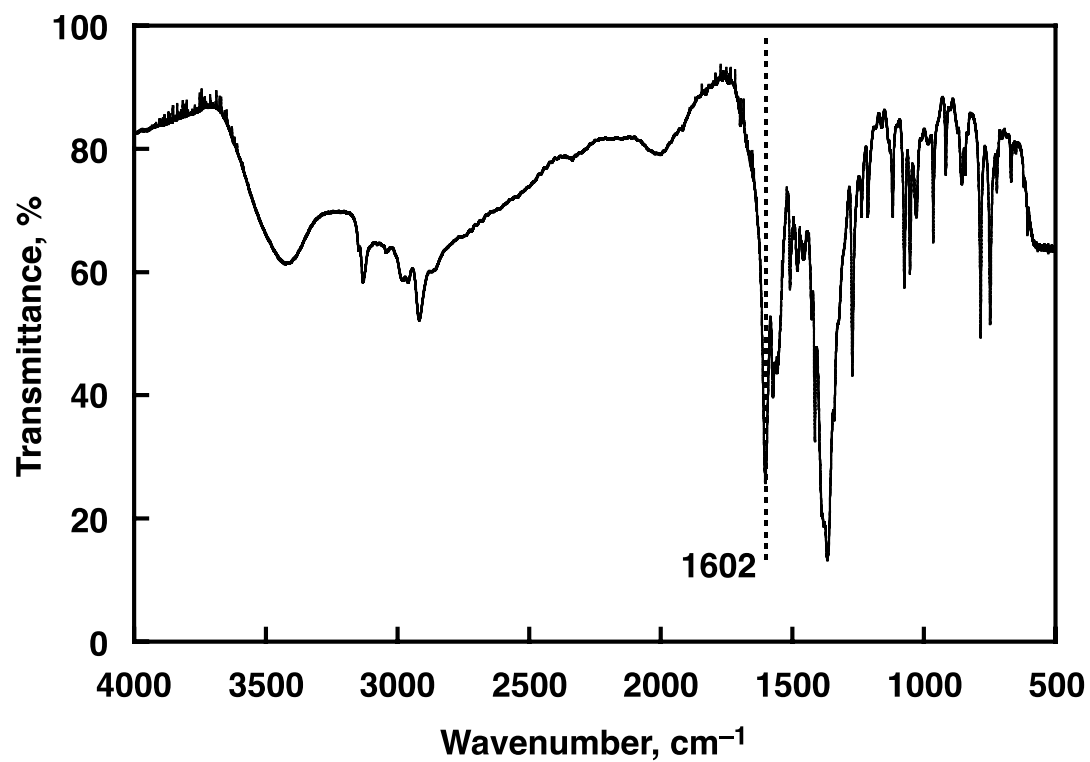


Fig. S12 IR spectrum of **2** diluted in a KBr disk.

Reference

1. Maenaka, Y.; Suenobu, T.; Fukuzumi, S. *J. Am. Chem. Soc.* DOI: 10.1021/ja207785f.